Interface Engineering in Quasi-Magnetic Tunnel Junctions with an Organic Barrier

Deung Jang Choi[†], Nyun Jong Lee, and Tae Hee Kim*

Department of Physics, Ewha Womans University, Seoul 120-750, Korea

Spin polarized tunneling through a hybrid tunnel barrier of a Spin filter (SF) based on a EuO ferro-magnetic semiconductor and an organic semiconductor (OSC) (rubrene in this case) was investigated. For quasi-magnetic tunnel junction (MTJ) structures, such as Co/rubrene/EuO/Al, we observed a strong spin filtering effect of the EuO layer exhibiting I-V curves with high spin polarization (P) of up to 99% measured at 4 K. However, a magnetoresistance (MR) value of 9% was obtained at 4.2 K. The low MR compared to the high P could be attributed to spin scattering caused by structural defects at the interface between the EuO and rubrene, due to nonstoichiometry in the EuO.

Keywords : spin filter, EuO, rubrene, Organic spintronics

1. Introduction

Organic materials have received considerable interest by researchers interested in spintronic applications due to the possibility of making flexible products with vastly different properties [1]. The most attractive aspect of OCSs for spintronic applications is their long spin relaxation lengths due to rather weak spin-orbit interactions: OSCs are composed of light elements like C, H, N, or O, all having a low atomic number (Z), and the spin-orbit coupling of these elements is proportional to Z^4. Long spin relaxation times in the order of a few tenths of micro seconds were obtained by different experimental techniques [2,3]. This advantage makes these materials ideal for spintronic applications. After Xiong *et al.*'s pioneering work, where a vertical spin valve with a tris(8-hydroxy-quinolinato)aluminum(Alq$_3$) organic barrier was realized [4], remarkable improvements have recently been achieved in the field of organic spin valve devices [5,6]. Barraud *et al.* observed an MR as large as 300% at 2 K in a La$_{0.7}$Sr$_{0.3}$MnO$_3$/Alq$_3$/Co tunnel junction, however a low MR of less than 5% was obtained at 180 K [6].

One important question arising in this field is to determine if OCSs can compete with inorganic semiconductor or metals in the development of realistic spintronic applications. It is not easy at this stage to answer whether

reasearch endeavours in organic spintronics will lead to their implementation in practical devices. Nevertheless, more challenges in both device performance and fundamental understanding of the mechanism affecting spin-related phenomena followed the first results reported by the researchers of the University of Utah. After all, it was clearly revealed that the choice of the electrode material is an important issue for spin injection into the organic layer since it determines the magnitude of the magneto-resistance. In a typical organic spin valve, half-metallic electrodes, such as La$_{0.7}$Sr$_{0.3}$MnO$_3$, are used as a spin emitter due to their perfect 100% spin polarization at low temperatures. Therefore, one can expect a high spin injection efficency from one ferromagnet to the other through the OSC barrier by taking advantage of the unimportant role of the conductive mismatch between metallic electrodes and the organic layer [7].

In this work, we investigated the spin transport properties with hybrid tunnel barrier junction structures, such as nonmagnetic metal (NM)/spin filter (SF)/organic semiconductor (OSC)/ferromagnet (FM). There is much interest in combining the spin filter effect with the adjacent OSC barrier. The spin filtering phenomenon can lead to highly spin-polarized (even up to 100%) charge carriers generated from non-magnetic electrodes and thus high tunneling magnetoresistance (TMR). Here, Al/EuO/Rubrene/Co/CoO magnetic tunnel junctions (MTJs) were studied. There are several reports about the spin filter effect of Eu chalcogenides, such as EuS, EuSe, and EuO [8-12]. Among

*Corresponding author: Tel: +82-2-3277-4647
Fax: +82-2-3277-2372, e-mail: taehee@ewha.ac.kr

these, we decide to use EuO as the spin filter material due to its larger exchange splitting energy and higher T_c (69.3 K) compared to the other Eu chalcogenides. We also utilized ruberene as an organic tunnel barrier due to its high charge carrier mobility and its large spin coherence length [13-17].

2. Experiment

We used a high vacuum deposition system to fabricate tunnel juncntions. The base pressure of this high vacuum chamber was 6×10^{-8} Torr. The MTJs were evaporated onto either glass substrates or Si substrates by thermal and e-beam evaporation. A mask system holding 8 different shadow masks was used for patterning the junctions. Film thickness was monitored *in situ* using a quartz crystal monitor. Overall 72 junctions of each type were prepared in a given run. The junction area was 200×200 μm^2.

As shown in Fig. 1, quasi-magnetic tunnel junctions with the hybrid tunnel barrier structure of 3.6 nm Al/EuO /rubrene/10 nm Co/CoO/6 nm Al_2O_3 were prepared.

The Al layer was formed on a liquid nitrogen cooled substrate in order to obtain a smooth structure. Then, the hybrid EuO and rubrene(Rub) tunnel barrier was deposited in sections at room temperature by thermal evaporation. EuO in particular was very carefully reactively evaporated in an oxygen partial pressure of 2×10^{-7} Torr. The thicknesses of 4 and 3.6 nm were deposited for EuO and Rub, respectively. After cooling down the substrate to 77 K, a 10 nm Co layer was deposited and was slightly oxidized at room temperature to form antiferromagnetic CoO on the surface in order to create the exchange bias for Co to fix its magnetization direction.

The typical technique used to study the transport properties of MTJs based on the conventional 4-point configuration is as follows. All transport measurements de-
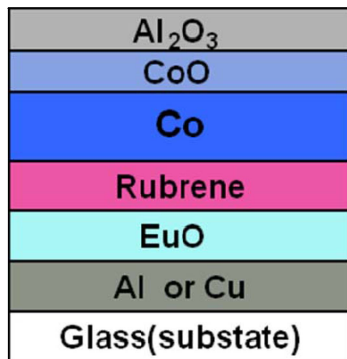
scribed in this study were performed with a home-built setup. This measurement system was equipped with a 0.8 Tesla magnet and temperature could be varied in the range of 4.2-300 K by flowing liquid helium and nitrogen to the cryostat. Temperature was adjusted using a temperature controller (Neocera, LTC-11). The equipment allowed the measurement of 4 junctions per run with a parallel or perpendicular magnetic field to the film plane.

3. Results and Discussion

The Junction Resistance (R_j) was measured using a conventional four probe configuration. The samples were directly dipped into a liquid Helium storage dewar for measuring the temperature dependence of resistance. The temperature was varied by adjusting the distance of the sample from the liquid helium level. Fig. 2 shows a drop of resistance at temperatures higher than the T_c of the bulk EuO (90 K), resulting from the difference of the non split barrier height and the exchange split barrier height. We expect a larger polarization for a sample exhibiting a larger resistance drop below its T_c. This MTJ exhibited a substantial resistance drop, indicating a large spin filter effect.

The current-voltage (I-V) characteristics for one MTJ are shown in Fig. 3. Non-ohmic behavior was observed, confirming that tunneling occurs through the EuO and rubrene hybrid tunnel barrier. Since this MTJ exhibited a non-linear behavior, such as normal, typical tunnel junctions, one can expect that NM and SF materials in quasi-MTJs act as FM electrodes in normal MTJs (FM/I/FM).

Using the tunneling model of Brinkman, Dynes, and Rowell (BDR) (eq. 1) [18], we can fit the I-V curves to extract the values of the mean tunnel barrier height (Φ),
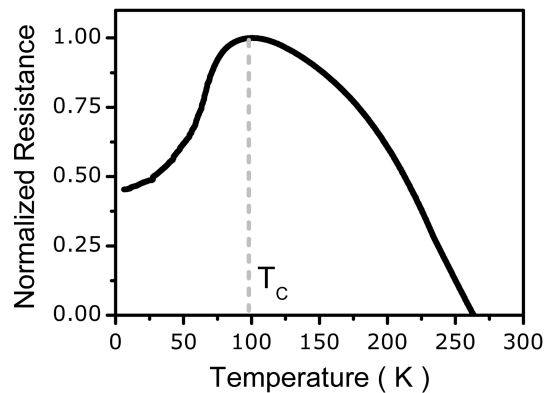

Fig. 1. Schematic diagram of the magnetic tunnel junction used for the second case.

Fig. 2. Temperature dependence of Normalized resistance for a 3.6 nm Al/4 nm EuO/3.6 nm Rub/10 nm Co/2.5 nm CoO/6 nm Al_2O_3 junction. The resistance dropped when the temperature goes down below the T_c.

barrier asymmetry ($\Delta\Phi$), and the barrier thickness (d). The BDR's J(V) equation is expressed as,

$$J(V)=G_0\left[V-\left(\frac{A_0\Delta\Phi}{32\Phi^{3/2}}\right)(eV)^2+\left(\frac{3A_0^2}{128\Phi}\right)(eV)^3\right]$$

$$G_0=\frac{e^2\sqrt{2m}}{(2\pi)^2\hbar^2}\left(\frac{\Phi^{1/2}}{d}\right)\exp\left(-\frac{2d}{\hbar}\sqrt{2m\Phi}\right), A_0=\frac{4d}{3\hbar}\sqrt{2m} \quad (1)$$

where J is the tunnel current density (A/cm^2), V is the voltage across the film (V), and e and m are the charge of an electron and the mass of an electron, respectively.

In the low bias region, eq. (1) was used to fit the I-V curve from −150 mV to +150 mV, giving the values of the barrier thickness (d), average barrier height (Φ), and its asymmetry ($\Delta\Phi$).

From the fit values of the barrier heights for the parallel state and anti-parallel state measured at 4 K, we obtained values of 0.046 eV, 0.160 eV, and 0.206 eV for the exchange splitting energy, $\Phi_\uparrow$, and $\Phi_\downarrow$ ($= \Phi_\uparrow + \Delta_{ex}$), respectively. The thickness d was found to be 78.3 Å. From these obtained values, we could then calculate the current density (J) for spin up and spin down using the BDR
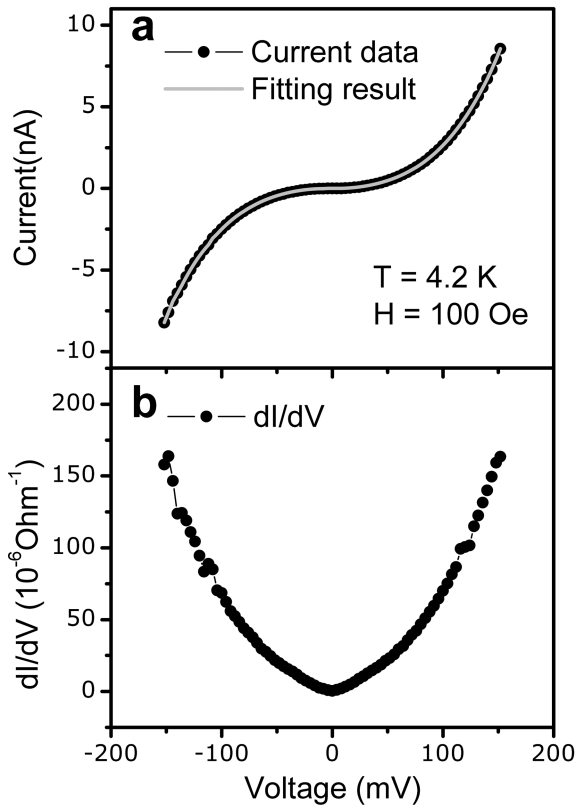

Fig. 3. I-V characteristics measured at 4.2 K for a 3.6 nm Al/ 4 nm EuO/3.6 nm Rub/10 nm Co/2.5 nm CoO/6 nm Al$_2$O$_3$ junction. a) The open circle and grey lines correspond to the current data and fitting result, respectively. b) dI/dV data.

equation. The values of $J_\uparrow$ and $J_\downarrow$ were determined to be 2.08×10^{-16} A/cm^2 and 3.68×10^{-18} A/cm^2, respectively. So, for the MTJ with a 3.6 nm thick rubrene barrier at 4.2 K, one can determine the polarization to be 99.4% from $P = (J_\uparrow - J_\downarrow) / (J_\uparrow + J_\downarrow)$.

The shape of conductance (dI/dV) versus bias is shown with a sharp dip at zero bias in Fig. 3-b). This means that the barrier and interfaces are influenced from magnetic inclusions. This is caused by the diffusion of magnetic impurities into the barrier [19].

The TMR was measured by a sweeping magnetic field between +2 kG and −2 kG to achieve the parallel and antiparallel states. The results were in good agreement with the M(H) curve, as shown in Fig. 4. Here, the TMR is defined as $\Delta R/R = (R_{AP} - R_P)/R_P$ [20, 21]. In Fig. 5-a), for this NM/EuO/OSC barrier/FM tunnel junction, a positive TMR was observed like a typical FM/I/FM MTJ, due to the spin polarization in EuO by spin filtering. As shown in Fig. 4-b), MRs of 1-9% were observed. These unexpectedly low values could be attributed to the imperfect interface structure between EuO and rubrene which might cause spin-incoherent scattering. According to Julliere's model [21], a 9% TMR suggests a P 11% for electrons crossing the EuO/rubrene hybrid barrier (P of ~40% assumed for Co). The bias dependence of the TMR for the same junction at 4.2 K is shown in Fig. 5-b). The TMR was persued even beyond 100 mV. A decrease of TMR as the bias voltage increases was observed and was attributed to the excitation of magnons, phonons, band effects, etc., at higher voltage regions [22, 23].

4. Summary

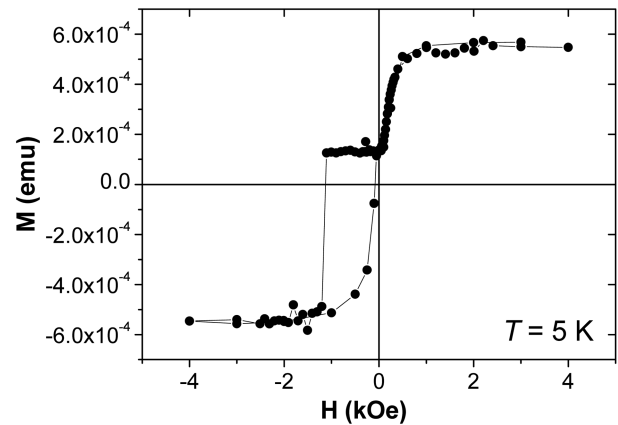In summary, we explored the spin transport properties

Fig. 4. M-H loop for a 1 nm Al/4 nm EuO/3.6 nm Rub/8 nm Co/2.5 nm CoO/6 nm Al$_2$O$_3$ multilayer measured at 5 K by a SQUID magnetometer.
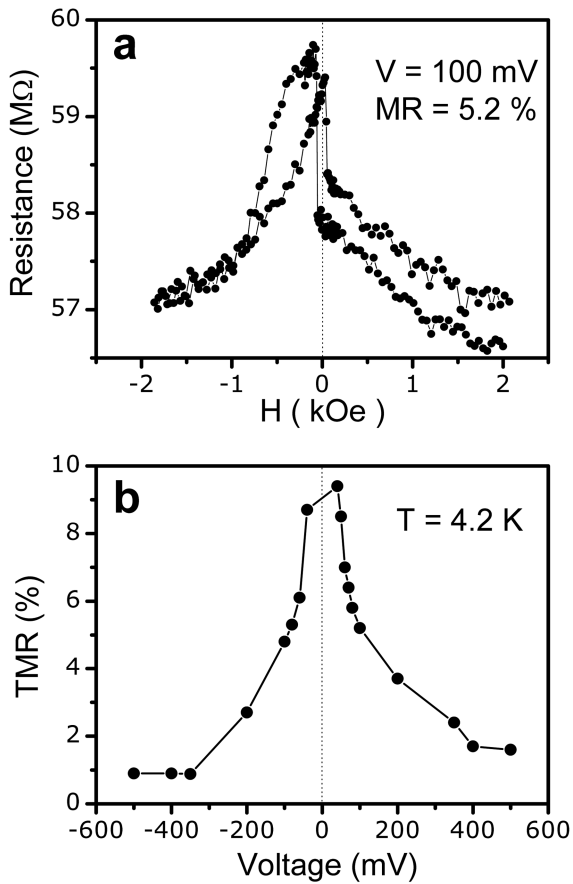
Fig. 5. Magneto-resistance curves measured at 4.2 K for the MR for a 3.6 nm Al/4 nm EuO/3.6 nm Rub/10 nm Co/2.5 nm CoO/6 nm Al_2O_3 junction. a) TMR measured with a 100 mV bias. b) Bias dependence of the TMR.

in a spin filter based on a EuO and organic semiconductor (rubrene) hybrid tunnel barrier. When we combined EuO with rubrene as a hybrid tunnel barrier, these junctions conserve the spin filter effect. We obtained the barrier height, barrier asymmetry, and thickness from the fitting of I (V) curves and calculated a P of 99.4%. Surprisingly, such a value was not associated with a high MR. Even though most importantly, from the above observation, we could conclude that there is a way to optimize the spin filtering effect by combining OSCs and, furthermore, it should be possible to inject spins even at room temperature into OSCs via a SF material. Electron spins can tunnel through a rubrene organic semiconductor tunnel barrier as observed in this work. We explored the influence of rubrene in a hybrid tunnel barrier with a EuO spin filter. Rubrene plays the role of magnetically decoupling the Co and EuO layers as well as the role of a tunnel barrier. It exhibited normal magnetic tunnel junction behavior. This behavior provides evidence that we can

use NM and SF materials as FMs of normal tunnel junctions. We obtain lower MR values compared to large P values. So it is worth trying to find the condition that gives big MRs with a hybrid tunnel barrier. For future work, we need to minimize spin scattering by optimizing the EuO and rubrene barrier and characterize the structure of the junction. Our work indicates the feasibility of developing new materials and techniques based on the spin transport phenomena through the organic barrier. By using organic materials in spintronic applications, new functionalities can be added to existing spintronic devices. For example, the multi-functionality achieved by using photons to control the spin current and vice versa could be achievable with OSCs. Predictions regarding the strong potential of organic spintronic devices are supported by the tremendous versatility to tune the electrical and magnetic behavior of organic materials by controlling their characteristics, including composition, dimension, and chemical potential.

References

[†] DJC's present address: Institut de Physique et Chimie des Materiaux de Strasbourg, UMR7504, 23 rue du Loess, BP43, 67034 Strasbourg Cedex 2, France.

[1] W. J. M. Naber, S. Faez, and W. G. van der Wiel, J. Phys. D: Appl. Phys. **40**, R205 (2007).

[2] C. B. Harris et al. Phys. Rev. Lett. **30**, 1019 (1973).

[3] V. I. Krinichnyi et al. Phys. Rev. B **55**, 16233 (1997).

[4] Z. H. Xiong, D. Wu, Z. V. Vardeny, and J. Shi, Nature (London) **427**, 821 (2004).

[5] T. Santos et al. Phys. Rev. Lett. **98**, 016601 (2007).

[6] C. Barraud et al. Nature Phys. **6**, 615 (2010).

[7] M. Yunus, P. P. Ruden, and D. L. Smith, J. Appl. Phys. **103**, 103714 (2008).

[8] J. S. Moodera, X. Hao, G. A. Gibson, and R. Meservey, Phys. Rev. Lett. **61**, 637 (1988).

[9] X. Hao, J. S. Moodera, and R. Meservey, Phys. Rev. B **42**, 8235 (1990).

[10] J. S. Moodera, R. Meservey, and X. Hao, Phys. Rev. Lett. **70**, 853 (1993).

[11] T. S. Santos and J. S. Moodera, Phys. Rev. B **69**, 241203(R) (2004).

[12] J. S. Moodera, T. S. Santos, and T. Nagahama, J. Phys.: Condens. Matter **19**, 165202 (2007).

[13] D. Käfer and G. Witte, Phys. Chem. Chem. Phys. **7**, 2850 (2005).

[14] D. D. Käfer, L. Ruppel, G. Witte, and Ch. Wöll, Phys. Rev. Lett. **95**, 166602 (2005).

[15] V. Podzorov, V. M. Pudalov, and M. E. Gershenson, Appl. Phys. Lett. **82**, 1739 (2003).

[16] A. F. Stassen, R. W. I. de Boer, N. N. Iosad, and A. F. Morpurgo, Appl. Phys. Lett. **85**, 3899 (2004).

[17] V. C. Sundar, J. Zaumseil, V. Podzorov, E. Menard, R. L. Willett, T. Someya, M. E. Gershenson, and J. A. Rogers, Science **303**, 1644 (2004).

[18] W. F. Brinkman, R. C. Dynes, and J. M. Rowell, J. Appl. Phys. **41**, 1915 (1970).

[19] J. Appelbaum, Phys. Rev. Lett. **17**, 91 (1966).

[20] J. S. Moodera, L. R. Kindera, T. M. Wong, and R. Meservey, Phys. Rev. Lett. **74**, 3273 (1995).

[21] M. Julliere, Phys. Lett. **54A**, 225 (1975).

[22] J. S. Moodera, J. Nowak, and R. J. M van de Veerdonk, Phys. Rev. Lett. **80**, 2941 (1998).

[23] J. S. Moodera and G. Mathon, J. Magn. Magn. Mater. **200**, 248 (1999); T. Nagahama, and J. S. Moodera, J. Magnetics **11**, 151 (2006).